Structures of hard-core Yukawa clusters and the tail-range dependence of the existence of a liquidlike cluster phase: Relevance to the physics of C_{60}

C. Rey and L. J. Gallego
Departamento de Física de la Materia Condensada, Facultad de Física, Universidad de Santiago de Compostela, Santiago de Compostela E-15706, Spain
(Received 28 March 1995)

The structures and melting behavior of hard-core Yukawa clusters from $N=2$ to $N=27$ particles were investigated by Monte Carlo simulations for several ranges of the attractive Yukawa tail. In contrast to Lennard-Jones clusters, the ground state configurations of hard-core Yukawa clusters with $N>13$ are of either hcp or fcc type, rather than icosahedral. The shortest tail range allowing a liquid phase in the cluster system is significantly longer than for bulk matter.

PACS number(s): 61.46.+w, 36.40.Ei

I. INTRODUCTION

Whether bulk C_{60} has a stable liquid phase has recently been the subject of some controversy [1–4]. Its existence, over a very narrow temperature range, has been predicted by Cheng, Klein, and Caccamo [1] (who used the integral equation theory and the molecular dynamics (MD) simulations) and by Mederos and Navascués [4] (who used the density-functional calculations), but Gibbs ensemble Monte Carlo (MC) simulations carried out in combination with free energy calculations and Clausius-Clapeyron integration suggest that no such liquid phase exists [2]. In all these studies, the potential used to describe the interaction between C_{60} molecules was that proposed by Girifalco [5], who successfully employed it to compute the second virial coefficient of the gas phase and certain crystal properties.

Whether a system has a stable liquid phase depends on the range of the attractive tail of the intermolecular potential; this was first shown by Gast, Hall, and Russel [6] for colloidal systems (for which corroboration has come from subsequent theoretical [7], experimental [8,9], and computer simulation [10] work), and for hard-core Yukawa (HCY) fluids (which successfully model a wide variety of real physical systems and have been extensively studied; see, e.g., Refs. [11–20]) has been confirmed by the theoretical and the Gibbs ensemble MC studies by Hagen and Frenkel [21] and Lomba and Almarza [22]. Hagen and Frenkel showed that the HCY fluids have no stable liquid phase if the range of the attractive tail is less than approximately one sixth of the hard core diameter. The limited temperature range of the liquid phase of the bulk C_{60} (if it exists) has accordingly been attributed to the relative weakness of the attractive tail of the Girifalco potential [1–4].

Free atomic and molecular clusters (small groups of atoms or molecules that before their eventual evaporation persist long enough for satisfactory characterization) have properties that often differ strikingly from those of bulk systems. In particular, solid-liquid coexistence has been studied in great detail in one-component clusters and is quite different from that of bulk matter (see, e.g., Ref. [23]). In view of the above-mentioned relationship between the attractive tail range of the potential and the existence of a bulk liquid phase, it is natural to inquire into the effect of the attractive interaction range on the existence of liquidlike states in small clusters, and compare this effect with the behavior of bulk fluids; as far as we know, no systematic studies of this question have been performed so far. It will be shown in this paper that, in general, the nonexistence of liquidlike clusters does not rule out the existence of a stable bulk liquid phase. Thus Rey, Gallego, and Alonso's [24] recent MD simulations of the clusters of C_{60} molecules using Girifalco's model, which showed a loss of C_{60} molecules by sublimation before liquidlike behavior could begin (in keeping with the experimental findings of Martin *et al.* [25]), do not necessarily support the prediction of Hagen *et al.* [2] that the bulk C_{60} has no liquid phase.

In this work we carried out MC simulations to investigate the melting behavior of small clusters of particles interacting via the HCY potentials of various tail ranges, and we compared our results with Hagen and Frenkel's [21] findings for the bulk HCY fluids. We also studied in detail the ground state structures of some of these clusters: above a certain very small size they are of either hcp or fcc type rather than icoshedral, which contrasts with the behavior of Lennard-Jones (LJ) clusters [26–28]. As indicated above, the properties of the bulk HCY systems have been extensively studied both theoretically and by computer simulations; the structure and dynamics of the HCY clusters, however, have not yet been investigated, and this paper is intended to fill, to a certain extent, this gap.

In Sec. II we describe the computational procedure used, in Sec. III we present and discuss our results, and in Sec. IV we briefly summarize the main conclusions.

II. DETAILS OF THE COMPUTER SIMULATIONS

We considered clusters of N identical particles interacting through a pairwise HCY potential of the form

 ©1996 The American Physical Society

$$v(r)=\begin{cases}\infty & (r<\sigma)\\ -(\varepsilon\sigma/r)\exp[-z(r-\sigma)] & (r\geq\sigma),\end{cases} \quad (1)$$

where σ is the diameter of the hard core of the particles, ε is the well depth, and the Yukawa exponent z is the inverse range parameter. Computations were carried out using reduced units, namely, σ for length, ε for energy, and $T^*=(kT/\varepsilon)$ for temperature, where k is the Boltzmann constant.

Canonical MC simulations were performed using the conventional Metropolis algorithm [29] with the clusters *in vacuo*. The maximum displacement was dynamically adjusted so as to give an acceptance ratio of 0.5. To obtain the low-temperature structures of the clusters, a high temperature ($T^*\approx 0.2$) run of 5×10^6 MC steps was first carried out, during which one configuration was recorded every 5×10^4 steps to obtain 100 uncorrelated initial configurations, to every one of which simulated quenching was applied by two different methods: (a) starting from the high-temperature initial configuration, a run was performed in which the temperature was slowly decreased every 10^6 steps to $T^*=10^{-8}$; (b) the same procedure as above, but now using as the starting configuration, after every temperature decrease, the structure of the lowest potential energy found until that stage. Procedure (b) is more efficient for finding the global minimum of the potential energy surface of a cluster. The double quenching process described above was repeated between four and ten times, depending on the cluster size.

To check the consistency of our structural results, two different test were carried out: (i) from the lowest energy structure of a cluster with N particles, the particle of the highest energy was removed to afford an $(N-1)$-particle cluster which was then cooled by procedure (b); (ii) to the lowest energy structure of a cluster with N particles, a new particle was added at a position minimizing the energy of the resulting $(N+1)$-particle cluster, which was then cooled by procedure (b). Although in some cases these tests yielded new local minima that had not been found by the double quenching method described in the previous paragraph, they confirmed that, unlike LJ clusters [26–28], several of the HCY clusters studied in this paper prefer geometries of either the hcp or fcc type; the reliability of these configurations was further tested by checking that they were those of the lowest energy among all possible hcp (fcc) arrangements containing the same number of particles. The extensive calculations performed make it highly probable that the lowest energy structures reported in this paper are indeed the ground state configurations of HCY clusters.

Starting from their ground state configurations, the melting behavior of the HCY clusters was investigated by gradually heating them to obtain their caloric curves. Evaporation was considered to have taken place when some atom had strayed farther than 5σ from the center of the mass of the cluster. For each temperature, the initial 5×10^6 or more configurations were discarded for equilibration, and the physical properties of interest were averaged over at least a further 10^7 configurations (both equilibration and equilibrium stages were longer for the largest clusters); at each temperature this was repeated at least four times so as to be able to estimate the statistical uncertainty of the average results (in the transition region, where large thermodynamic fluctuations occur, up to ten repetitions were carried out). In addition to the mean configurational energy $\langle U\rangle$, we calculated the relative root-mean-square (rms) pair separation fluctuation δ and the configurational heat capacity C as functions of temperature, using the expressions [30]

$$\delta=\frac{2}{N(N-1)}\sum_{i<j}\frac{(\langle r_{ij}^2\rangle-\langle r_{ij}\rangle^2)^{1/2}}{\langle r_{ij}\rangle} \quad (2)$$

and

$$C=\frac{\langle U^2\rangle-\langle U\rangle^2}{kT^2}, \quad (3)$$

where r_{ij} is the distance between particles i and j and the angle brackets indicate averages over one MC simulation after equilibration. The quantities δ and C reflect melting and other "softening" thermal mechanisms.

III. RESULTS AND DISCUSSION

We investigated the HCY clusters in the size range $N=2$–27 for several values of the reduced inverse range parameter $z^*=z\sigma$ of the attractive Yukawa tail. In particular, we discuss here our results for the z^* values 1.8 and 3.9. The former has been used in studies of the pure HCY fluid [11,13,18] because it makes this system qualitatively like a LJ fluid as regards the densities and temperatures of the liquid in equilibrium with its vapor; and the latter value (3.9) has been employed by Hagen and Frenkel [21] in their study of the bulk HCY systems because it makes the Boyle temperature of the HCY system equal to that of C_{60} as modeled by Girifalco's potential.

A. Ground state configurations

For $N=5$–27, Table I lists the calculated binding energies (i.e., the reduced configurational energies per particle, but with the opposite sign) for low-temperature icosahedral, hcp and fcc HCY clusters with $z^*=1.8$ (for $N=2$–4) the binding energies are those of 2, 3, and 4 particles in contact with each other: 0.5, 1, and 1.5, respectively). For $N=5$–13, the most stable configurations are icosahedral, as in the case of the LJ clusters [26–28]. In particular, the ground state configurations of the 5-, 6-, 7- and 13-particle HCY clusters are, respectively, the trigonal bipyramid, the square bipyramid, the pentagonal bipyramid, and the icosahedron. This latter structure is shown in Fig. 1 together with the corresponding metastable hcp and fcc geometries. It should be noted that the 13-particle icosahedral configuration is slightly distorted in order to maximize the number of contacts.

For $N>13$, icosahedral structures are unstable, and when allowed to relax adopt nonicosahedral structures with smaller binding energies than those of the hcp and fcc configurations. In the size range $N=14$–19 the preferred configurations are of the hcp type (Table I), and

are formed by successively adding particles to the 13-particle hcp core of Fig. 1(b) at the positions indicated by the arrows in Figs. 2(a)–2(f). For comparison, Figs. 3(a)–3(f) show the configurations of the competing fcc structures, which have slightly lower binding energies. The fcc clusters are generally formed by successively adding particles (at the positions indicated by the arrows in Fig. 3) to the 13-particle fcc structure of Fig. 1(c). However, this growth sequence is interrupted at $N=19$, the configuration of the 19-particle fcc cluster being derived from the 13-particle fcc cluster by adding six particles at the positions indicated by the crosses in Fig. 3(f). In the size range $N=20-22$, the most stable configurations are fcc, the 20- and 21-particle clusters being derived by successively adding particles to the 19-particle fcc cluster at the positions indicated in Figs. 3(g) and 3(h), and the 22-particle cluster by adding nine particles to the 13-particle fcc cluster at the positions indicated by the crosses in Fig. 3(i) (the second cross on one of the particles indicates an unseen added particle behind the visible particle). Figures 2(g)–2(i) show the metastable (energetically competitive) hcp geometries in the size range $N=20-22$. The 20-particle hcp cluster is the 19-particle hcp cluster plus an extra particle at the position indicated by the arrow in Fig. 2(g). However, the 21- and 22-particle hcp configurations correspond to different arrangements in which the successive layers of the clusters have 3, 8, 7, and 3 particles ($N=21$) or 7, 8, and 7 particles ($N=22$).

TABLE I. Binding energies for low-temperature icosahedral, hcp, and fcc HCY clusters with $z^*=1.8$. For $N>13$, icosahedral structures are unstable and lose icosahedral symmetry when allowed to relax. Note that for $N=5$, "icosahedral" ≡hcp; for $N=6$, "icosahedral" ≡hcp ≡fcc; and for $N=7$ and $N=8$, hcp≡fcc.

N	icosahedral	hcp	fcc
5	1.839 194	1.839 194	1.734 197
6	2.167 746	2.167 746	2.167 746
7	2.411 829	2.352 891	2.352 891
8	2.563 370	2.533 686	2.533 686
9	2.768 296	2.689 399	2.683 488
10	2.933 926	2.897 753	2.882 079
11	3.091 511	3.075 737	3.001 078
12	3.270 051	3.183 676	3.165 869
13	3.433 933	3.403 697	3.402 453
14		3.527 159	3.527 076
15		3.647 225	3.640 592
16		3.746 603	3.745 085
17		3.845 818	3.838 058
18		3.928 960	3.925 292
19		4.013 665	4.012 627
20		4.068 760	4.080 686
21		4.145 547	4.146 199
22		4.251 192	4.257 556
23		4.327 172	4.320 838
24		4.435 422	4.420 512
25		4.499 100	4.464 136
26		4.596 342	4.507 583
27		4.628 218	4.545 182

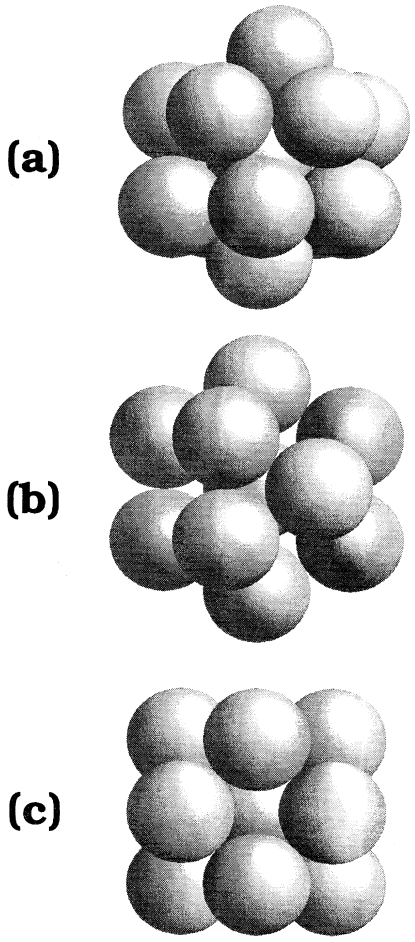

FIG. 1. Low-temperature structures of the 13-particle HCY cluster with $z^*=1.8$: icosahedral (a), hcp (b), and fcc (c).

In the size range $N=23-27$ the ground state configurations are again hcp (Table I), growing by successive additions of single particles to the 22-particle hcp cluster as illustrated for $N=23$ in Fig. 2(j). The competing 23-particle fcc cluster [Fig. 3(j)] also derives from the corresponding 22-particle configuration.

The geometries of the HCY clusters with $z^*=1.8$ thus differ from those of the LJ clusters, which are all icosahedral up to $N\approx5000$ [26–28]. Moreover, cluster stability peaks at $N=7$, 13, 22, 24, and 26 (as indicated by the prominent peaks in a plot of the second finite differences of the lowest reduced configurational energy as a function of cluster size; Fig. 4), whereas MD simulations [31] of the LJ clusters in the size range $N=7-33$ predict peak stabilities for the 13-, 19-, and perhaps 7-atom clusters, whose structures are the icosahedron, the double icosahedron, and the pentagonal bipyramid, respectively. The structural differences between the HCY and LJ clusters arise because the LJ potential has a softer repulsive wall and a broader potential well than the HCY potential (Fig. 5): at low temperature, the preferred separation of the LJ particles differs from that of the HCY particles, giving rise to different cluster configurations.

HCY clusters with $z^*=3.9$ have the same structures as those with $z^*=1.8$ (Table II), except that the most stable configuration for $N=23$ is of the fcc rather than the hcp type. Moreover, the 13-particle cluster with $z^*=3.9$ is no longer more stable than all those of neighboring sizes (Fig. 6); and for larger z^* (shorter potential tail ranges) the 13-particle HCY cluster becomes hcp instead of icosahedral.

B. Melting

The systems simulated in this work, small clusters *in vacuo*, are of course thermodynamically unstable and will eventually evaporate, but before evaporating they can persist long enough for simulations to allow satisfactory characterization of quasiequilibrium states and of processes such as melting. No real time scale can be given for the melting processes observed in this work because the MC method ignores time, but the stability of the small clusters is illustrated by the results obtained for the LJ clusters, whose properties have been extensively studied by MD simulations. Román and Garzón [32], for instance, found that at all points of the caloric curve the

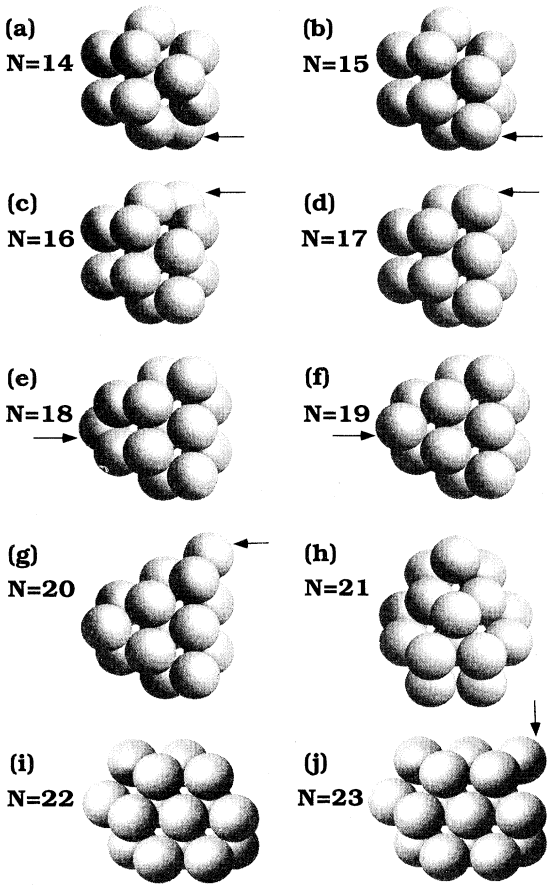

FIG. 2. Low-temperature geometries of the hcp type for some HCY clusters with $N>13$ and $z^*=1.8$. Arrows indicate the cluster construction sequence (see text).

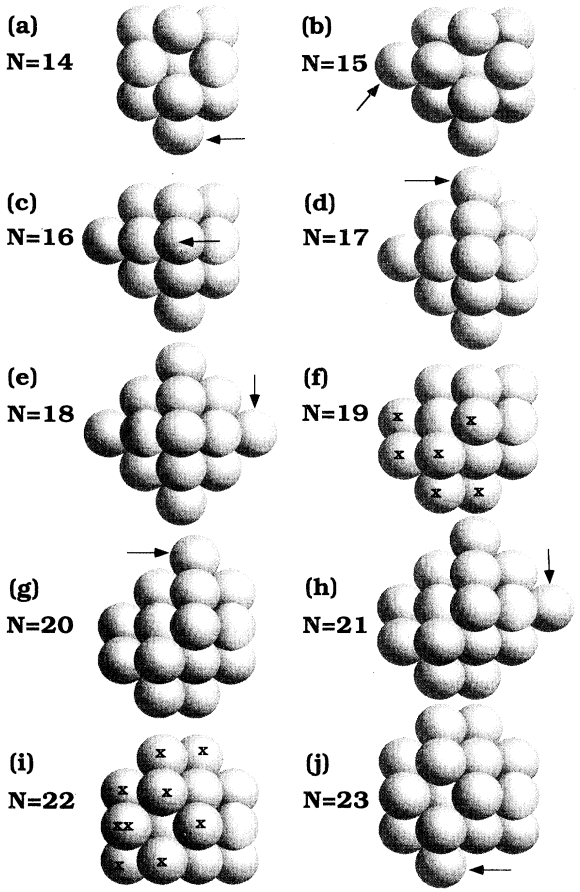

FIG. 3. Low-temperature geometries of the fcc type for some HCY clusters with $N>13$ and $z^*=1.8$. Arrows and crosses indicate the cluster construction sequence (see text).

13-atom LJ clusters were stable (i.e., did not evaporate) for at least 10^5 simulation time steps of $0.01\times 2^{1/6}\sigma(m/\varepsilon)^{1/2}$, which would amount to 2.4 ns for Ar_{13} (for further details, see papers by Román and Garzón [32] and Rey *et al.* [33], who computed the survival probabilities of the small LJ clusters as a function of time in states situat-

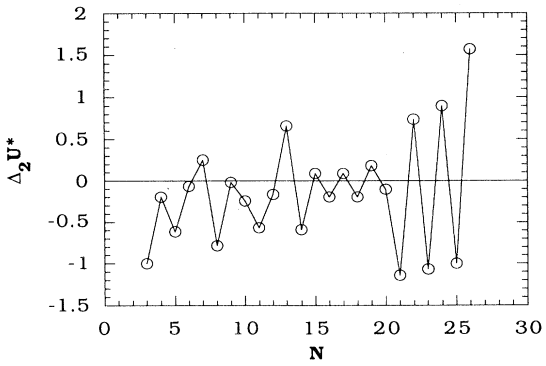

FIG. 4. Second finite differences of the lowest reduced configurational energy $(\Delta_2 U^*(N)=U^*(N+1)+U^*(N-1)-2U^*(N))$ as a function of the cluster size for the HCY clusters with $z^*=1.8$.

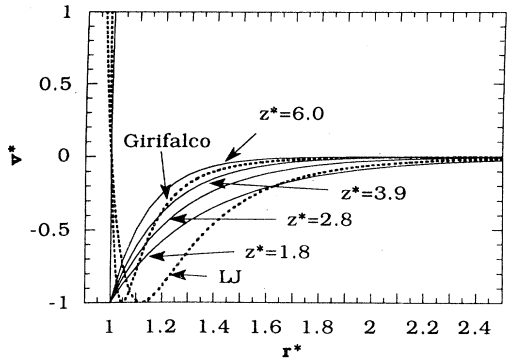

FIG. 5. A comparison of the HCY potential for several values of the inverse range parameter z^* (continuous curves) and the LJ and Girifalco potentials (dotted curves). The potential energy is expressed in units of the well depth and the intermolecular distance in terms of the distance at which the potential crosses zero (for C_{60}, $\varepsilon/k = 3218$ K and $\sigma = 0.959$ nm).

ed in both the solid-liquid coexistence and liquidlike regions of the caloric curves). To gain further assurance that the results obtained in this work correspond to systems in quasiequilibrium, the caloric curves were computed both by heating from low temperature and by cooling the clusters from temperatures close to evaporation. In all cases we found that the caloric curves obtained on cooling closely fit those obtained under heating. There was no detectable hysteresis within the fluctuations in the transition regions.

We investigated the melting behavior of several sizes of

TABLE II. As for Table I, but for HCY clusters with $z^* = 3.9$.

N	icosahedral	hcp	fcc
5	1.810 373	1.810 373	1.656 230
6	2.070 288	2.070 288	2.070 288
7	2.293 652	2.217 345	2.217 345
8	2.399 811	2.345 210	2.345 210
9	2.546 557	2.454 162	2.445 786
10	2.666 627	2.625 361	2.620 321
11	2.773 425	2.766 353	2.683 641
12	2.890 660	2.820 177	2.814 804
13	2.983 292	2.966 109	2.965 012
14		3.059 878	3.059 505
15		3.144 602	3.142 074
16		3.216 177	3.214 954
17		3.282 383	3.279 277
18		3.338 958	3.337 015
19		3.392 308	3.392 095
20		3.432 340	3.437 980
21		3.456 202	3.479 978
22		3.532 297	3.540 079
23		3.574 950	3.576 498
24		3.655 299	3.651 548
25		3.689 649	3.678 341
26		3.759 819	3.703 462
27		3.779 961	3.726 353

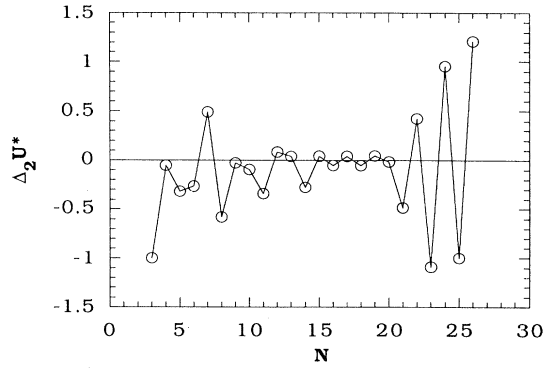

FIG. 6. As for Fig. 4, but for $z^* = 3.9$.

the HCY clusters, but for the sake of brevity only the results for the 13-particle cluster are reported here. Figure 7 shows the calculated caloric, δ, and specific heat curves for the case $z^* = 1.8$. Melting is shown by the sharp rise of δ from small values indicating a rigid, solidlike cluster at $T^* < 0.17$ to much larger values indicative of a nonrigid, liquidlike form. This transition is also reflected by the

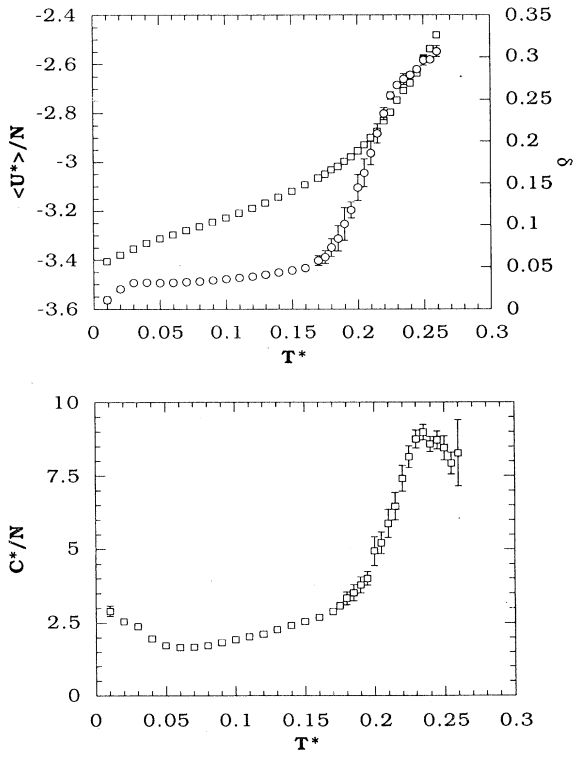

FIG. 7. Melting behavior of the HCY cluster with $N = 13$ and $z^* = 1.8$. In the upper panel, squares represent the reduced mean configurational energy per particle (left-hand scale), circles the relative rms pair separation fluctuation (right-hand scale). In the lower panel, squares represent the reduced configurational specific heat. Error bars are shown for the δ and specific heat results. The statistical uncertainty in the energy is about 0.01% in the solidlike region, increasing to 0.3% at the end of the caloric curve.

strong peak in the specific heat curve. In the temperature range between the beginning and the end of the jump in δ ($0.17 < T^* < 0.23$) solidlike and liquidlike clusters coexist, as is shown by the configurational energy distribution being fitted by the sum of the two Gaussian components (Fig. 8) [34]. Over the range $0.23 < T^* < 0.26$ clusters are in a fully liquidlike state, and at $T^* = 0.26$ evaporation takes place.

The behavior of the 13-atom HCY cluster with $z^* = 3.9$ is significantly different (Fig. 9). In this case, evaporation occurs during the melting transition, and the specific heat curve shows no melting peak. The maximum value of z^* for which the 13-particle HCY cluster has a liquidlike phase is about 2.8. The corresponding caloric, δ, and specific heat curves are shown in Fig. 10. When the inverse range parameter z^* is larger than 2.8, evaporation of the 13-particle HCY cluster takes place before it can attain a fully liquidlike state. Calculations for the HCY clusters with a larger number of particles, within the range studied in this paper, gave similar results.

The above melting results contrast with Hagen and

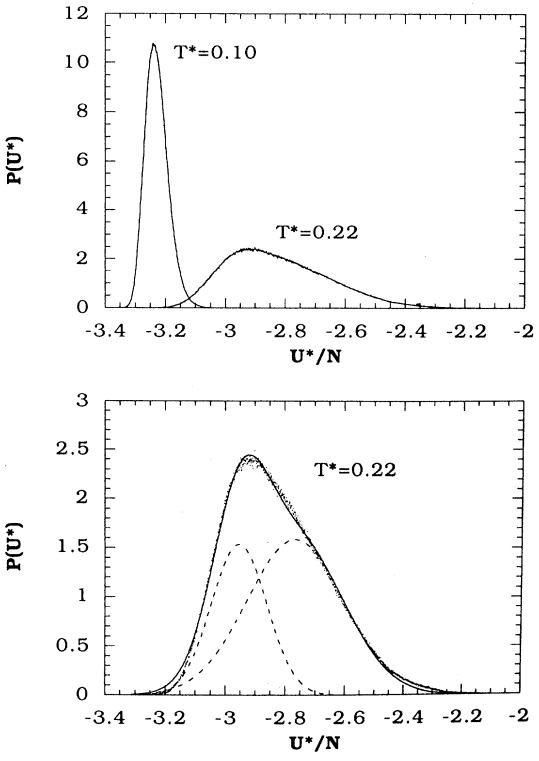

FIG. 8. Configurational energy distribution for the 13-particle HCY cluster with $z^* = 1.8$. $P(U^*)$ is the normalized probability density. In the upper panel we show the distributions at two different temperatures: at $T^* = 0.1$, i.e., in the solidlike region, the distribution is approximately Gaussian; the $T^* = 0.22$ distribution corresponds to the coexistence region. In the lower panel, the solid line represents the best fit to the distribution data points at $T^* = 0.22$ (small dots), which was obtained as the sum of two overlapping Gaussian distributions (dashed curves).

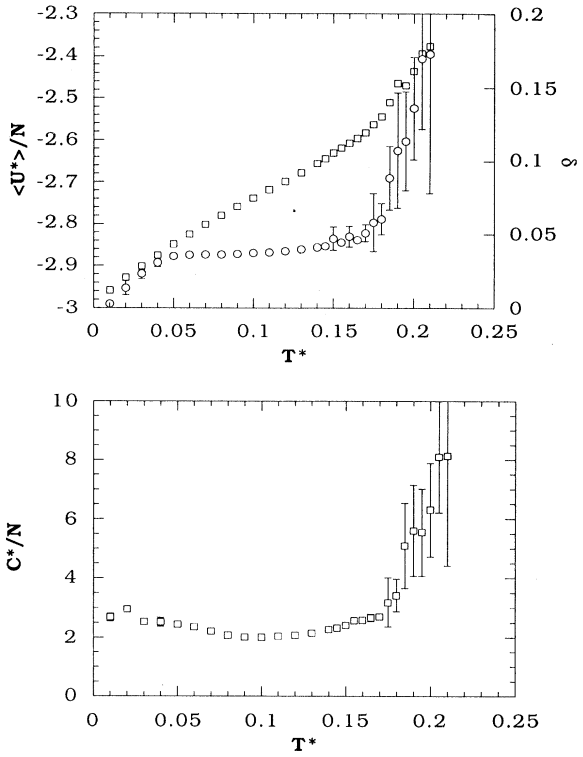

FIG. 9. As for Fig. 7, but for $z^* = 3.9$ (the statistical uncertainty in the energy at the end of the caloric curve is, in this case, of the order of 1%).

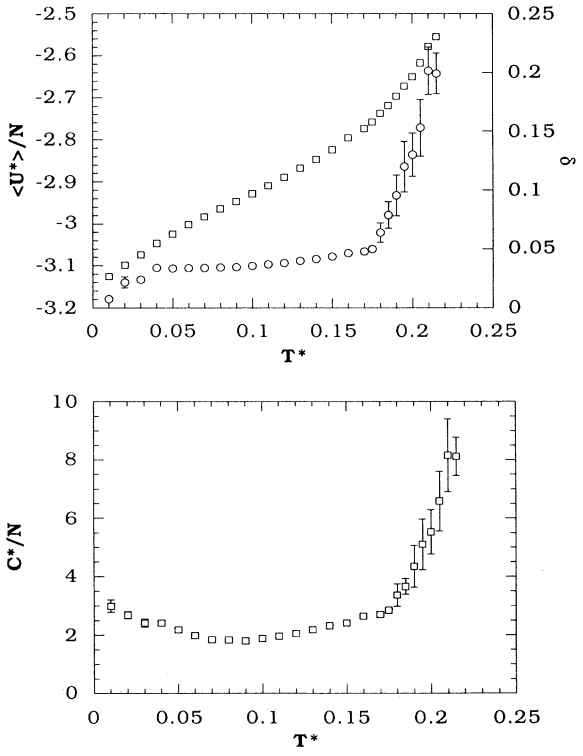

FIG. 10. As for Fig. 7, but for $z^* = 2.8$ (the statistical uncertainty in the energy at the end of the caloric curve is, in this case, of the order of 0.5%).

Frenkel's [21] finding that the bulk HCY systems have no stable liquid phase if z^* is larger than approximately six. Liquid states are therefore feasible in the bulk HCY system for shorter potential tail ranges than in the case of the small clusters. More specifically, within the range $2.8 < z^* < 6$ HCY clusters of the sizes studied in this paper have no quasistable liquidlike form (because evaporation occurs before melting), but stable bulk liquid states are possible. This difference arises from the fact that most of a cluster's particles are located at the surface of the cluster, as a result of which they can readily escape through thermal agitation (which is what it means to say that free clusters are thermodynamically unstable). What we have seen is that, although free clusters will always evaporate eventually, they can be stable enough to exhibit melting before evaporation takes place provided that the range of the attractive part of the intermolecular potential is long enough to supply the cohesive energy necessary to quasistabilize the liquidlike phase. Our results show that the shortest tail range allowing a quasistable liquidlike phase in small clusters is significantly longer than the shortest tail range allowing a stable liquid phase for the bulk matter (Fig. 5).

In view of the above, the nonexistence of the liquidlike clusters is not necessarily incompatible with the existence of a stable bulk liquid phase. Fullerene C_{60} may be a case in point. Figure 5 shows that the range of the Girifalco potential for C_{60} is significantly shorter than the shortest HCY range allowing the HCY clusters to attain a liquidlike state, which suggests that as the temperature is increased fullerene clusters should lose C_{60} molecules by sublimination before liquidlike behavior begins. This is in keeping with the results of the recent experimental [25] and computer simulation [24] studies of this kind of cluster. However, the range of the Girifalco potential is longer than (although very close to) Hagen and Frenkel's [21] estimate of the shortest HCY range allowing the bulk HCY systems to possess stable liquid states. This suggests that the bulk C_{60} may perhaps have a stable bulk liquid phase, which would agree with the calculations of Cheng, Klein, and Caccamo [1] and Mederos and Navascués [4]. The fact that the range of the Girifalco potential is very close to that of the HCY potential for $z^* = 6$ indicates that C_{60} is, in fact, a borderline case for the existence of a bulk liquid phase, which is consistent with the discrepancies among different attempts to predict whether C_{60} does or does not have such a phase [1–4].

Figure 5 also shows that the attractive tail of the LJ interaction decays more slowly than that of the HCY potential for $z^* = 2.8$ (and, therefore, for $z^* = 6$). The implication of this, that both cluster and bulk LJ systems have a liquid phase, is fully borne out by the results of the computer simulations of the LJ systems (see, e.g., Refs. [23] and [35]).

IV. SUMMARY AND CONCLUSIONS

In this work we studied the structures and melting behavior of the HCY clusters from $N = 2$ to $N = 27$ particles for several ranges of the attractive Yukawa tail. In contrast to the LJ clusters, the ground state geometries of either the hcp or fcc type are energetically preferred to the icosahedral configurations for the HCY clusters with $N > 13$. The minimum of the HCY potential being located at the hard-core distance, zero-temperature HCY structures are close-packed arrangements in which the particles tend to maximize the number of contacts.

Simulation of the behavior of these clusters as the temperature is raised shows that the shortest attractive Yukawa interaction range allowing the existence of a liquid phase is significantly longer for the clusters than for the bulk system. Hence the nonexistence of the liquidlike clusters is not necessarily incompatible with the existence of a stable bulk liquid phase. In view of the results of Rey, Gallego, and Alonso [24] for clusters of the C_{60} molecules and of Cheng, Klein, and Caccamo [1] and Mederos and Navascués [4] for bulk C_{60}, fullerene may be a case in point.

ACKNOWLEDGMENTS

This work was supported by the DGICYT, Spain (project No. PB92-0645-C03-03) and the Xunta de Galicia (project No. XUGA20602B92). Facilities provided by the Galician Supercomputer Center (CESGA) are also acknowledged.

[1] A. Cheng, M. L. Klein, and C. Caccamo, Phys. Rev. Lett. **71**, 1200 (1993).
[2] M. H. J. Hagen, E. J. Meijer, G. C. A. M. Mooij, D. Frenkel, and H. N. W. Lekkerkerker, Nature (London) **365**, 425 (1993).
[3] N. W. Ashcroft, Nature (London) **365**, 387 (1993).
[4] L. Mederos and G. Navascués, Phys. Rev. B **50**, 1301 (1994).
[5] L. A. Girifalco, J. Phys. Chem. **96**, 858 (1992).
[6] A. P. Gast, C. K. Hall, and W. B. Russel, J. Colloid Interface Sci. **96**, 251 (1983).
[7] H. N. W. Lekkerkerker, W. C.-K. Poon, P. N. Pusey, A. Stroobants, and P. B. Warren, Europhys. Lett. **20**, 559 (1992).
[8] P. N. Pusey, W. C.-K. Poon, S. M. Ilett, and P. Barlett, J. Phys. Condens. Matter **6**, A29 (1994).
[9] F. Leal Calderón, J. Bibette, and J. Biais, Europhys. Lett. **23**, 653 (1993).
[10] E. J. Meijer and D. Frenkel, Phys. Rev. Lett. **67**, 1110 (1991).
[11] D. Henderson, E. Waisman, J. L. Lebowitz, and L. Blum, Mol. Phys. **35**, 241 (1978).

[12] A. P. Copestake, R. Evans, H. Ruppersberg, and W. Schirmacher, J. Phys. F **13**, 1993 (1983).
[13] G. A. Mansoori and N. Kioussis, J. Chem. Phys. **82**, 2076 (1985).
[14] J. Th. G. Overbeek, in *Physics of Complex and Supermolecular Fluids,* edited by S. A. Safran and N. A. Clark (Wiley, New York, 1987).
[15] E. Arrieta, C. Jedrzejek, and K. N. Marsh, J. Chem. Phys. **86**, 3607 (1987).
[16] D. J. González and M. Silbert, J. Phys. F **18**, 2353 (1988).
[17] H. M. van Horn, Science **252**, 384 (1991).
[18] C. Rey, L. J. Gallego, and L. E. González, J. Chem. Phys. **96**, 6984 (1992).
[19] C. Rey, L. J. Gallego, L. E. González, and D. J. González, J. Chem. Phys. **97**, 5121 (1992).
[20] C. Rey, L. E. González, L. J. Gallego, and D. J. González, J. Chem. Phys. **100**, 560 (1994).
[21] M. H. J. Hagen and D. Frenkel, J. Chem. Phys. **101**, 4093 (1994).
[22] E. Lomba and N. G. Almarza, J. Chem. Phys. **100**, 8367 (1994).
[23] S. Sugano, *Microcluster Physics* (Springer-Verlag, Berlin, 1991).
[24] C. Rey, L. J. Gallego, and J. A. Alonso, Phys. Rev. B **49**, 8491 (1994).
[25] T. P. Martin, U. Näher, H. Schaber, and U. Zimmermann, Phys. Rev. Lett. **70**, 3079 (1993).
[26] J. D. Honeycutt and H. C. Andersen, J. Phys. Chem. **91**, 4950 (1987).
[27] B. W. van de Waal, J. Chem. Phys. **90**, 3407 (1989).
[28] M. R. Hoare and P. Pal, J. Cryst. Growth **17**, 77 (1972).
[29] M. P. Allen and D. J. Tildesley, *Computer Simulation of Liquids* (Oxford University Press, Oxford, 1990).
[30] H. L. Davis, J. Jellinek, and R. S. Berry, J. Chem. Phys. **86**, 6456 (1987).
[31] T. L. Beck, J. Jellinek, and R. S. Berry, J. Chem. Phys. **87**, 545 (1987).
[32] C. E. Román and I. L. Garzón, Z. Phys. D **20**, 163 (1991).
[33] C. Rey, L. J. Gallego, M. P. Iñiguez, and J. A. Alonso, Physica B **179**, 273 (1992).
[34] J. Jellinek, T. L. Beck, and R. S. Berry, J. Chem. Phys. **84**, 2783 (1986).
[35] J. A. Barker and D. Henderson, Rev. Mod. Phys. **48**, 587 (1976).

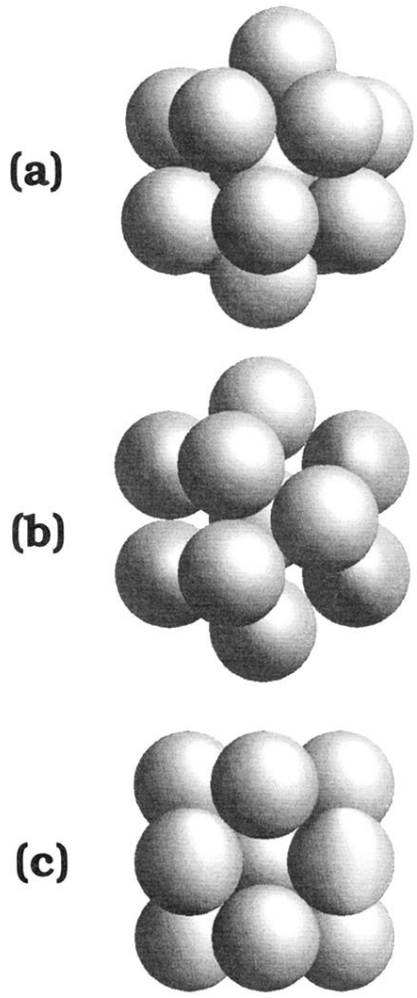

FIG. 1. Low-temperature structures of the 13-particle HCY cluster with $z^* = 1.8$: icosahedral (a), hcp (b), and fcc (c).

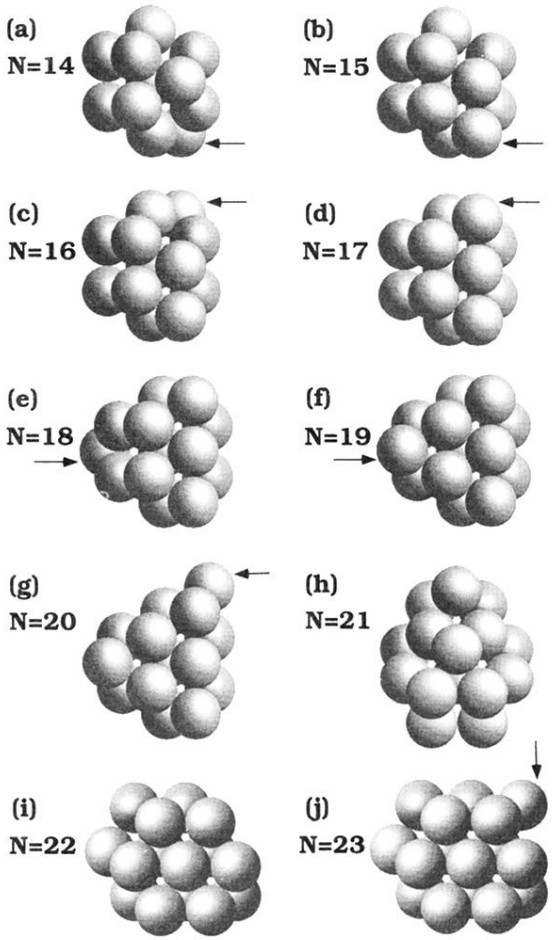

FIG. 2. Low-temperature geometries of the hcp type for some HCY clusters with $N > 13$ and $z^* = 1.8$. Arrows indicate the cluster construction sequence (see text).

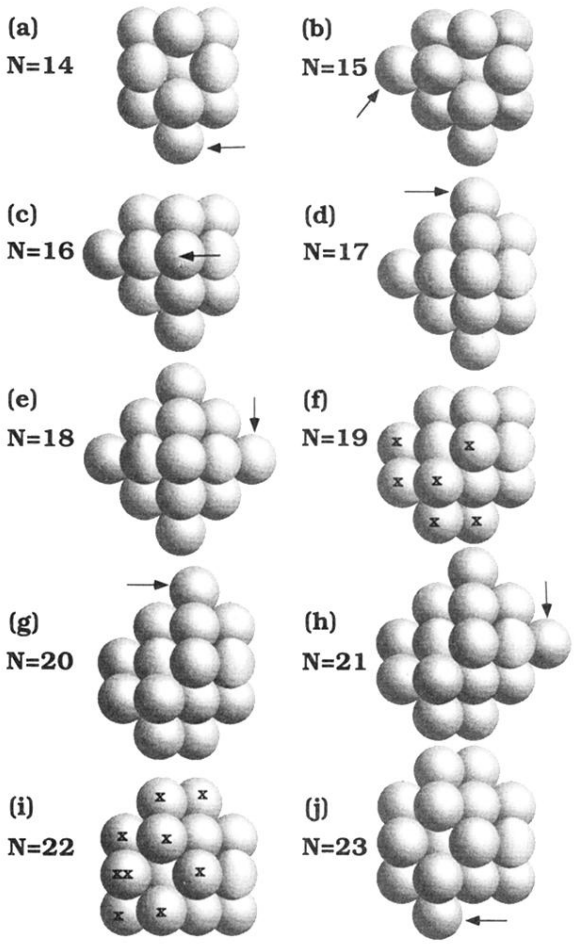

FIG. 3. Low-temperature geometries of the fcc type for some HCY clusters with $N > 13$ and $z^* = 1.8$. Arrows and crosses indicate the cluster construction sequence (see text).